REVIEW ARTICLE

THORACIC INVOLVEMENT IN SYSTEMIC PRIMARY VASCULITIS: RADIO-LOGICAL PATTERNS AND FOLLOW-UP

G. Serra, A.-L. Brun, D. Toledano, P. Cluzel, P.A. Grenier[1]

Systemic primary vasculitides are rare idiopathic diseases causing an inflammatory injury to the vessel walls. A pulmonary involvement is frequent, and chest-CT is the imaging technique of reference in its assessment. An extremely wide variety of parenchymal, vascular and airways abnormalities, has been described and diagnosis can be challenging: knowledge of clinical data and a close cooperation with the referring physician is often crucial. The aim of this work is to describe the most common typical and atypical CT features of pulmonary vasculitis and their possible changes over time and therapy, focusing on the differential diagnosis with other inflammatory/infectious or neoplastic diseases.

Key-words: Lung, CT – Vasculitis.

Systemic primary vasculitis is a group of idiopathic diseases in which the sole or predominant histological feature is primarily represented by an inflammatory insult to the vessel walls with vessel destruction.

The nomenclature and classification of vasculitis have been proposed in 1994 and revisited in 2012 by the International Chapel Hill Consensus Conference (CHCC) on the Nomenclature of Systemic Vasculitides (1, 2). This classification is based on the size of vessels principally involved (large, medium and small).

Although the exact pathogenesis of vasculitis is still matter of discussion and research, an immunological dysfunction is highly suspected, as suggested by many clinical, pathological and serological data derived from affected patients (3, 4). Also genetic and environmental factors (drugs or infectious microorganisms) would play a key role in the genesis and development of disease. Three main immunological mechanisms of vessel damage have been identified and the genesis of each vasculitis would be primarily based on deposition of immune complexes, antibody-mediated vascular disease, and/or cell-mediated immunity and granulomatous reaction. In particular, the investigations on the antibodies directed against peri-nuclear and cytoplasmatic neutrophil components (ANCA: antineutrophil cytoplasmatic antibodies) allowed the identification of a sub-group of ANCA-associated vasculitis charac-

terized by similar clinical features, involvement of small vessels and response to immunosuppressive treatment (4).

Pulmonary involvement can be identified in all systemic vasculitides. However in this review we will consider only primary systemic vasculitis that are most frequently accompanied by lung involvement.

Small vessel-vasculitis is divided into ANCA-associated vasculitis (AAV) and immune complex small vessel vasculitis. AAV is a necrotizing vasculitis with few or no immune deposits that predominantly affects small vessels and is associated with myeloperoxidase ANCA (MPO-ANCA) or proteinase 3 ANCA (PR3-ANCA). AAV is subdivided into microscopic polyangiitis (MPA), granulomatosis with polyangiitis (GPA, formerly Wegener's granulomatosis) and eosinophilic granulomatosis with polyangiitis (EGPA, formerly Churg Straus syndrome).

Immune complex-small vessel vasculitis is characterized by moderate to marked vessel wall deposits of immunoglobulines and complement components that predominantly affects small vessels. Glomerulonephritis is frequently seen among the diseases included in this group. We will review anti-glomerulo basement membrane (anti GBM) disease (formerly Goodpasture syndrome) which may affect lung parenchyma.

This review will include also Takayashu arteritis and Behçet disease classified into large-vessel vas-

culitis and variable-vessel vasculitis respectively.

Clinical signs and symptoms

They are variable and non specific. Small-vessel vasculitis can cause fever, myalgias, arthralgias, and malaise. A multiple organ systems involvement can be found, with various clinical scenarios such as renal failure, uveitis, sinus disease, shortness of breath and rashes. Such clinical associations should always rise the suspicion of a small-vessel vasculitis when another cause is still unknown.

Large-vessel vasculitis can cause clinical signs and symptoms related to ischemia and unexplained inflammatory syndromes. Since overlapping imaging features and similar clinical presentations are very common, the differential diagnosis among the different vasculitis or other inflammatory/infectious and neoplastic diseases can be extremely challenging. For these reasons, a deep knowledge of the peculiar imaging patterns of each disease, integrated with the patient's clinical background derived from a close cooperation with the referring clinician, is necessary to achieve the correct diagnosis.

CT imaging features of pulmonary vasculitis

When assessing a chest-CT in a case of suspect vasculitis, the radiologist may face an incredibly wide spectrum of imaging presentations, ranging from no abnormality (no pulmonary involvement) to extensive lung disease (3, 4). When detected, a lung involvement can derive from pathological abnormalities affecting
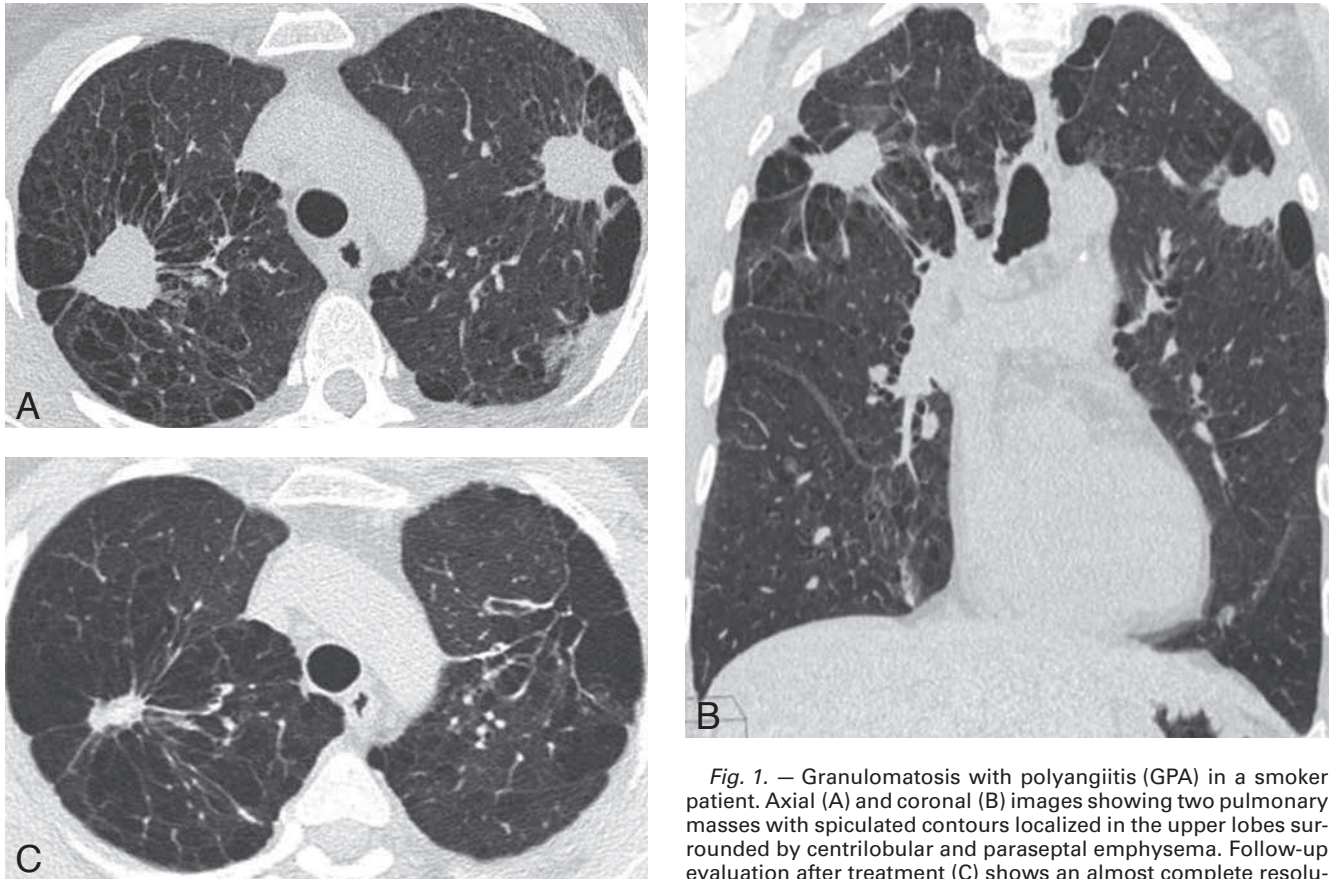
Fig. 1. — Granulomatosis with polyangiitis (GPA) in a smoker patient. Axial (A) and coronal (B) images showing two pulmonary masses with spiculated contours localized in the upper lobes surrounded by centrilobular and paraseptal emphysema. Follow-up evaluation after treatment (C) shows an almost complete resolution on pulmonary masses with residual fibrotic linear changes.

any anatomical or functional component of the lung: vessels (pulmonary and/or systemic), parenchyma, airways (trachea and bronchi) and pleura. The main imaging patterns suggesting a lung involvement are represented by parenchymal nodules and masses (with or without cavitations), diffuse or focal ground-glass opacities, parenchymal consolidations, tracheal or bronchial abnormalities (wall thickening, stenosis), vascular abnormalities (aneurysms, wall thickening, stenosis and inflammation), interstitial lung disease and pleural disease. Recently a non fortuitous association with pulmonary fibrosis has come to evidence, especially in ANCA-associated vasculitis (5).

Although overlapping patterns are very common, characteristic imaging features and their associations can help distinguish between diseases (6-8). In this process, the knowledge of the clinical background of the patient is crucial. Moreover, each abnormality can show significant changes over time, related to the natural evolution of disease (acute versus chronic) and therapeutic interventions, which can also lead to a complete resolution with no residual abnormality.

Granulomatosis with polyangiitis (GPA)

GPA is necrotizing granulomatous inflammation usually involving the upper and lower respiratory tract, and necrotizing vasculitis predominantly affects small to medium vessels.

It is a rare multi-organ disease (prevalence of 3/100.000 in the USA) (2), which can affect all ages but is most common in adults 50-69 years of age; men are slightly more frequently affected than women. All organs can be affected; the most frequently affected sites are the upper respiratory tract (sinusitis and nasal ulceration), kidneys and lower respiratory tract. The lower respiratory tract (airways and lungs) is affected in 90% of patients.

Radiological manifestations of the disease (9-11)

The most typical radiological manifestation of lung disease at chest-CT is represented by nodules and masses (90% of cases) (Fig. 1A, B). In active disease, nodules are expression of granulomatous inflammation and necrosis, with tendency towards cavitation. Nodules dimension ranges from few millimeters to masses of 10 cm, the margins are more commonly smooth than irregular, the nodules are frequently bilateral (75% of cases), with random distribution and no lobar predilection. Occasionally they show a predominant or exclusive peripheral (subpleural) distribution, or, less commonly, have a peribronchovascular localization. The halo-sign (a non specific rim of ground-glass opacity surrounding the pulmonary lesion) may be detected in up to 15% of nodules, and may express perinodular hemorrhage and/or inflammation. After contrast media administration, a hypoattenuated area in the core of the nodule may be identified as expression of central necrosis. In a small number of cases a feeding vessel can also be seen. Calcifications are rare.

With progression of disease nodules tend to increase in number and size, and cavitation is common in nodules greater than 2 cm (50% of cases).

Cavitations are usually thick-walled and show irregular inner margins; less frequently, and often after therapy, they can show thin and smooth walls; sometimes an air-full level can be detected.
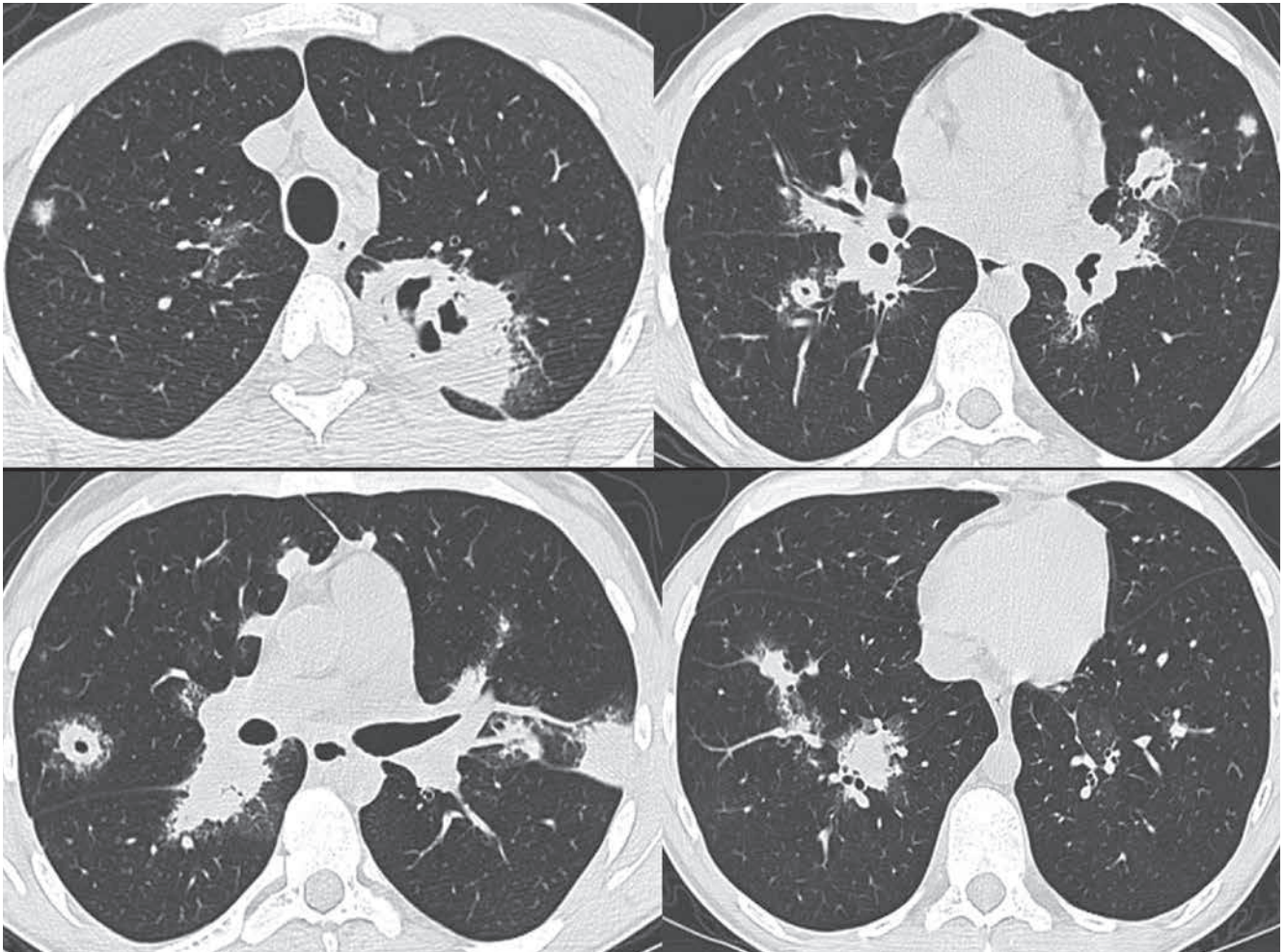
Fig. 2. — GPA in a 23-year-old patient presenting with multiple pulmonary nodules and masses associated with airspace consolidation areas having a peribronchovascular and peripheral distribution. Some of the nodules and masses are cavitated. Most of the lesions are surrounding by a rim of ground-glass opacity (halo-sign).
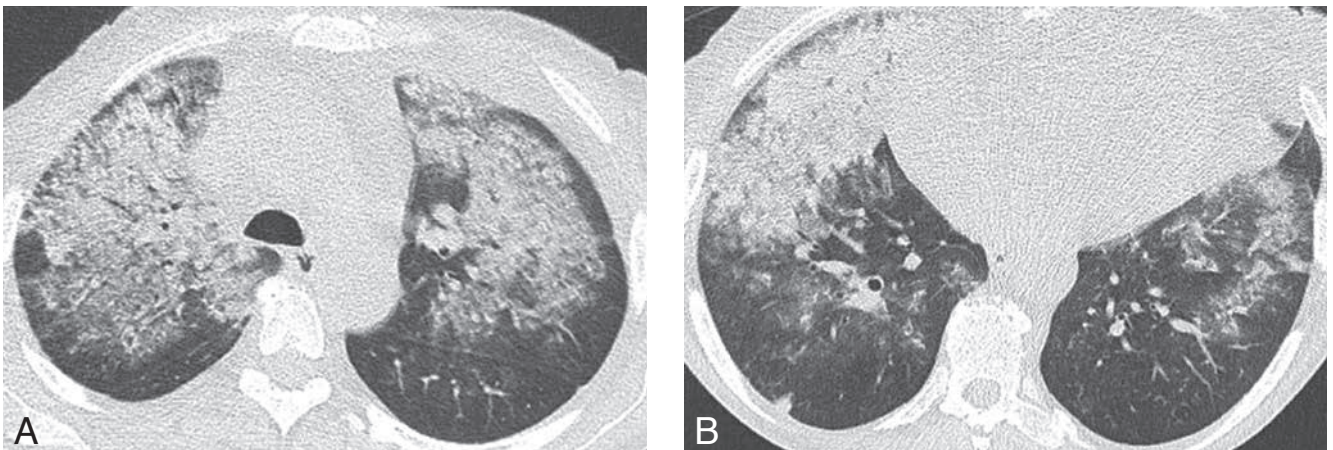

Fig. 3. — GPA patient presenting with recurrent hemoptysis. Axial images showing bilateral airspace consolidation, associated with some ground-glass opacities mainly located in the upper and anterior parts of the lungs.

The second most common radiological manifestation is represented by airspace consolidations (25%–50% of cases), which may occur with or without nodules and masses (Fig. 2). Patchy or diffuse ground-glass opacities are seen less commonly (20%-30% of cases). Both airspace consolidation and ground-glass opacities may reflect either vasculitic pulmonary disease in the form of pneumonitis or alveolar hemorrhage. Areas of consolidations usually show a random distribution; sometimes they appear as subpleural wedge-shaped lesions mimicking pulmonary infarcts, or have a peribronchial distribution.
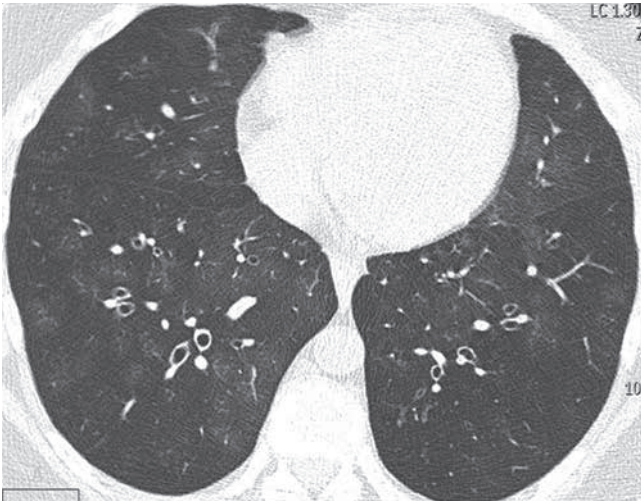
Fig. 4. — CT study in a GPA patient presenting with recurrent episodes of hemoptysis showing diffuse centrilobular areas of ground-glass opacity reflecting pulmonary hemorrhage.

lobe in extension (Fig. 3). Bilateral, diffuse ground-glass opacities may be seen in a small proportion of patients. In a small number of cases centrilobular small nodules (Fig. 4) of variable density and branching linear opacities (« tree in bud » pattern), septal and intralobular linear opacities (reticular pattern) have been described. Rarely, pulmonary fibrosis with typical usual interstitial pneumonia (UIP) pattern (bilateral subpleural honeycombing) may occur. Pleural effusions, unilateral or bilateral and of variable extent are quite uncommon In a small proportion of patients (15%) hilar and/or mediastinal lymph node enlargement can be detected.

Airspace consolidations are characterized by quite variable shapes and appearances, ranging from dense and localized abnormalities to bilateral, patchy or confluent consolidations, sometimes involving a whole

Tracheal and bronchial involvement is a common manifestation in GPA being reported in up to the 15%-25% and 40-70% of patients respectively (12,13). Nodular appearance of inner surface of the airways may occur (Fig. 5). Tracheal stenoses are usually subglottic (this area should
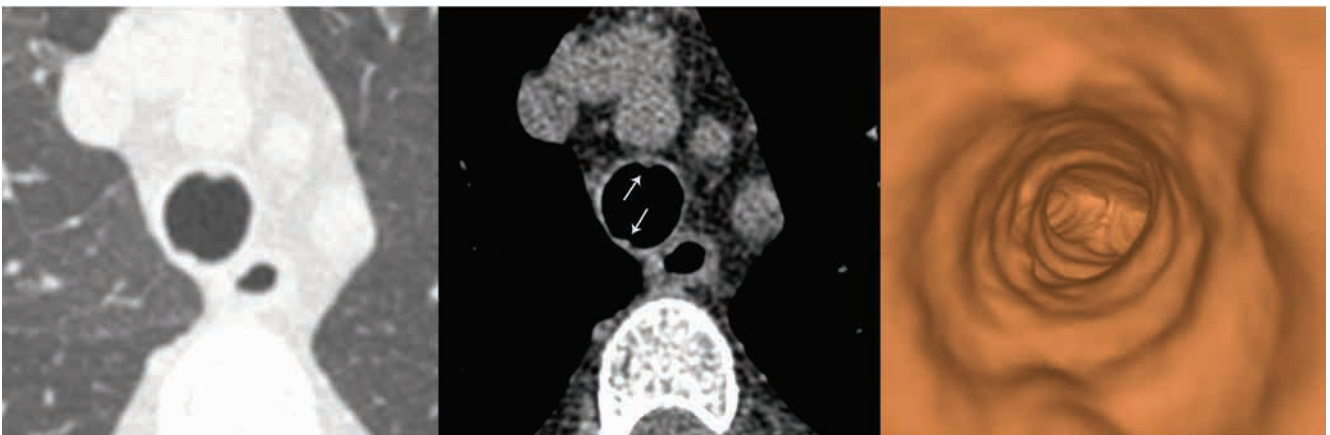

Fig. 5. — Tracheal involvement in a patient with GPA. CT study shows the presence of a nodular appearance of the inner surface of the trachea detected on lung parenchymal (left) and mediastinal (middle) window settings. This is confirmed on virtual bronchoscopic descending view (right).
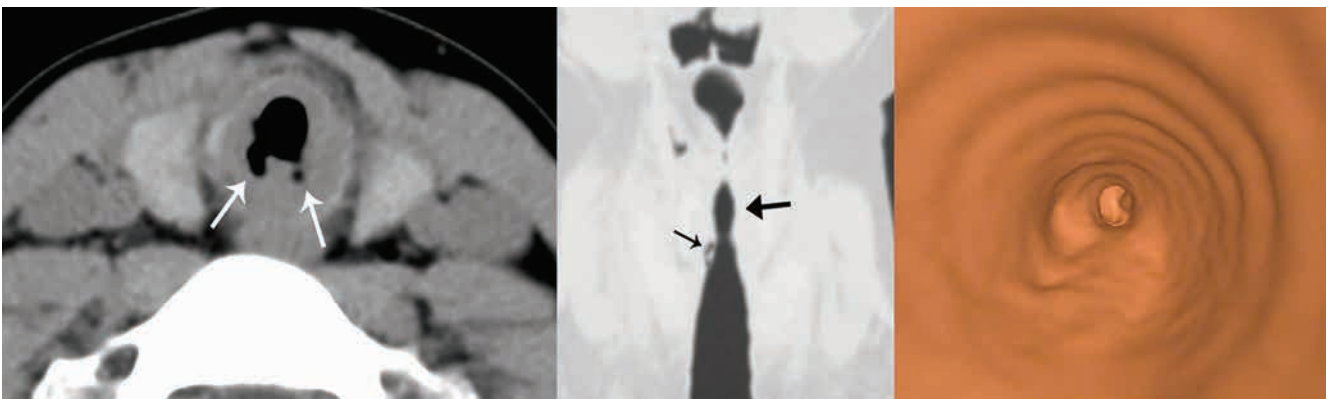

Fig. 6. — Patient affected by GPA with airway involvement. CT shows subglottic concentric stenosis of the tracheal lumen. The image on the left axial image shows a circumferential thickening of the tracheal wall and two posterior fistulae (arrows). The coronal oblique reformation with minimum intensity projection (middle) shows the concentric smooth stenosis in the subglottic location (arrow), and a small fistula (small arrow). The virtual endoscopic view of the stenosis shows the symmetric appearance of the stenosis (right).
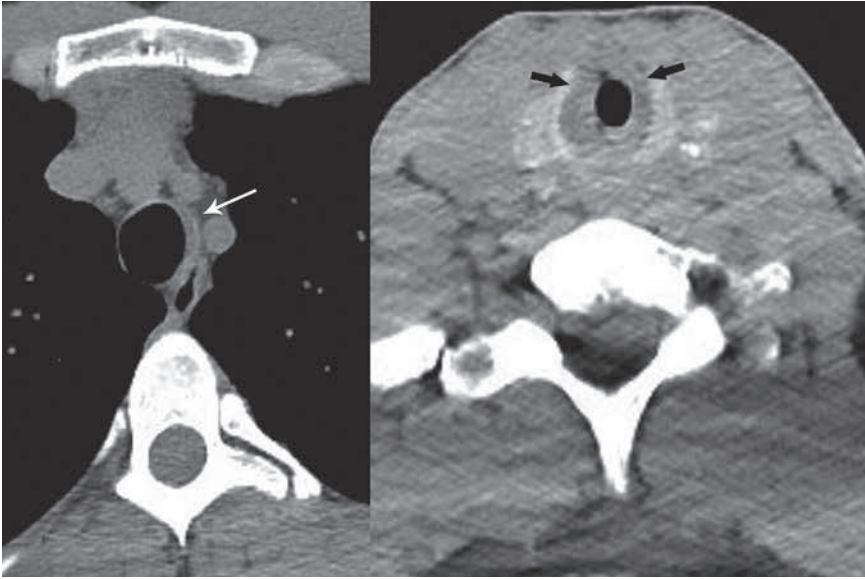
Fig. 7. — Airway involvement in a patient with GPA. The left axial image shows an asymmetrical tracheal wall thickening. The right axial image shows a circumferential thickening of the tracheal wall with narrowing of the lumen (subglottic stenosis).
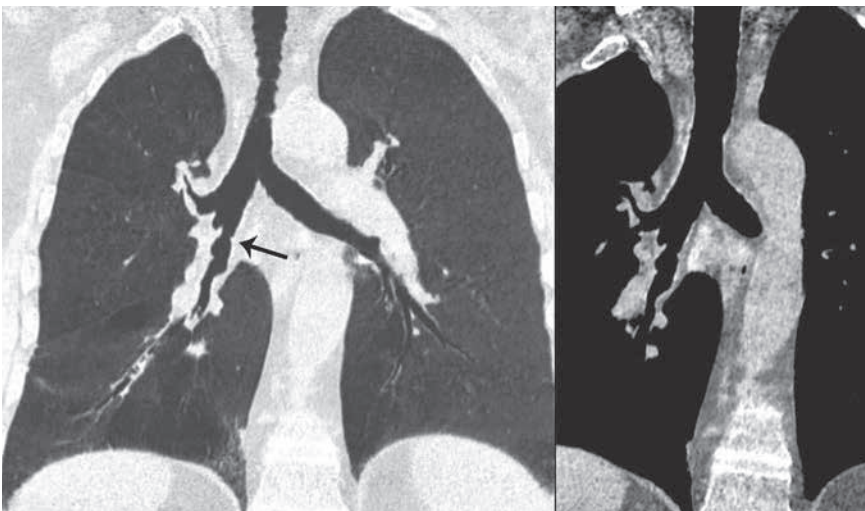

Fig. 8. — Patient with GPA. Coronal reformatted slab with minimum intensity projection (left) and contrast enhanced coronal reformation with mediastinal window settings (right). Stenosis (arrow) and irregularity of the inner surface of the right intermediate and lower bronchi. Contrast enhancement of bronchial walls reflecting the presence of active inflammation.
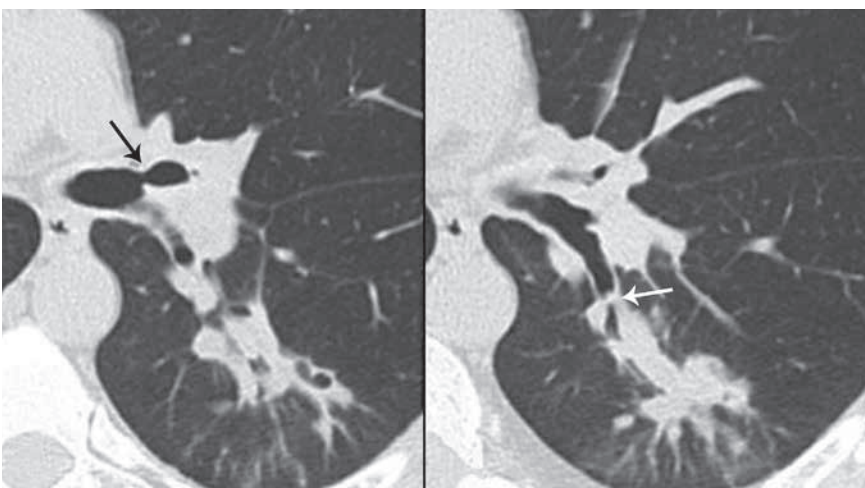
always be included in the study acquisition volume), can be smooth or irregular, most commonly circumferential and about 2-4 cm long (Fig. 6 and 7).

The tracheal rings can show calcifications, thickening and cartilaginous erosions. Mucosal thickening may be symmetrical or asymmetrical, irregular or ulcerated. Fistulas may be present (Fig. 6). A possible involvement of the vocal cords must be assessed. Any bronchus (lobar, segmental and subsegmental) may be involved. Segmental and subsegmental bronchial walls can be thickened and lumen stenotic (Fig. 8, 9 and 10), resulting in possible airway obstruction and atelectasis.

Bronchiectasis (Fig. 10) and patchy air trapping can be found in the 10%-20% and 30% of cases respectively.

Imaging Follow-up

Follow-up studies after therapy (immunosuppressive treatment) can show, in the majority of cases, a complete resolution of ground-glass opacities and nodules and a decrease in size or complete resolution of the masses (Fig. 1C and 11) (14). Cavitated lesions may develop in thin-walled cavitations. A reduction of tracheal or bronchial wall thickening can be observed as well (Fig. 12). Fibrotic changes (intralobular linear opacities and septal thickening) and bronchiectasis tend to remain stable.

Differential diagnosis

The main radiologic differential diagnoses include other diseases (particularly infections and neoplasms) that may essentially result in airspace consolidation, multiple nodules and masses, with or without cavitations. The knowledge of the clinical background of the patient (upper respiratory symptoms, laboratory data suggesting a glomerulonephritis and presence of serum ANCA) is essential in the formulation of diagnosis. Septic embolism or multiple lung abscesses are usually associated with bacteremia and tend to involve mainly the lower lobes and are rarely

Fig. 9. — Bronchial involvement in a patient with GPA. On the left, there is a short concentric luminal narrowing of the origin of the left upper lobar bronchus (arrow), and on the right, an occlusion of the superior segmental bronchus of the left lower lobe (arrow) with peripheral peribronchovascular consolidation.
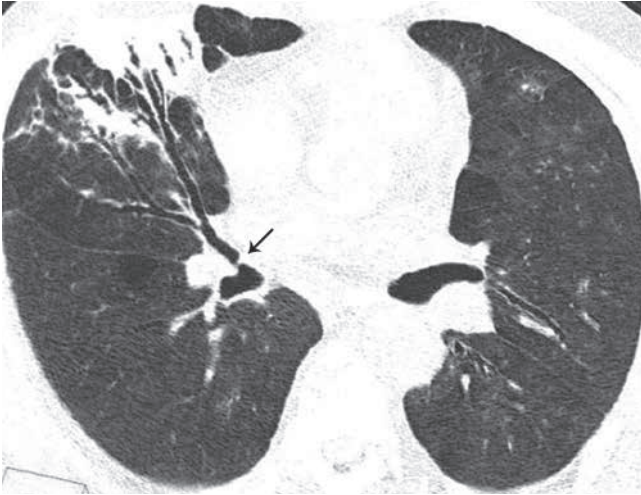
Fig. 10. — Subsegmental bronchiectasis and distal airspace consolidation in the same patient as figure 8. Stenosis of the origin of the right middle lobar bronchus (arrow).

greater than 3 cm. Hematogeneous metastases mainly involve the lower lobes. Cavitations are uncommon in lymphoma and rapid changes of nodules and masses dimensions and distribution, often observed in GPA, argue against malignancy.

Eosinophilic granulomatosis with polyangiitis (EGPA)

EGPA is eosinophil-rich and necrotizing granulomatous inflammation often involving the respiratory tract, and necrotizing vasculitis predominantly affects small to medium vessels and is associated with asthma and eosinophilia (2). ANCA is more frequently seen in EGPA when glomerulonephritis is present. It is a very rare disease (annual incidence: 1-3/million), mainly affecting middle-aged patients (40-50 years old), clinically characterized by asthma and allergic rhinitis, peripheral hypereosinophilia and necrotizing vasculitis, virtually present in all cases (15,16).

Radiological manifestations of the disease

The most common imaging feature (present in up to 90% of cases) is represented by bilateral areas of ground-glass opacities or consolidations (Fig. 13). Their distribution is usually symmetric, with a peripheral predominance and no lobar predilection; less commonly, they have a peribronchial or patchy random distribution.

- Septal lines can be seen in approximately 50% of cases. The interlobular septal thickening can be explained either by the presence of edema secondary to cardiac involvement or by an eosinophilic infiltration of the septa.

- Nodules or masses with dimensions ranging from few millimeters to 3.5 cm are uncommon, with or

Fig. 11. — Follow-up evaluation in the same patient as figure 2. Resolution after treatment of the peribronchovascular consolidation of the right upper lobe, and cavitated mass of the left upper lobe after treatment, with some residual linear fibrotic changes.
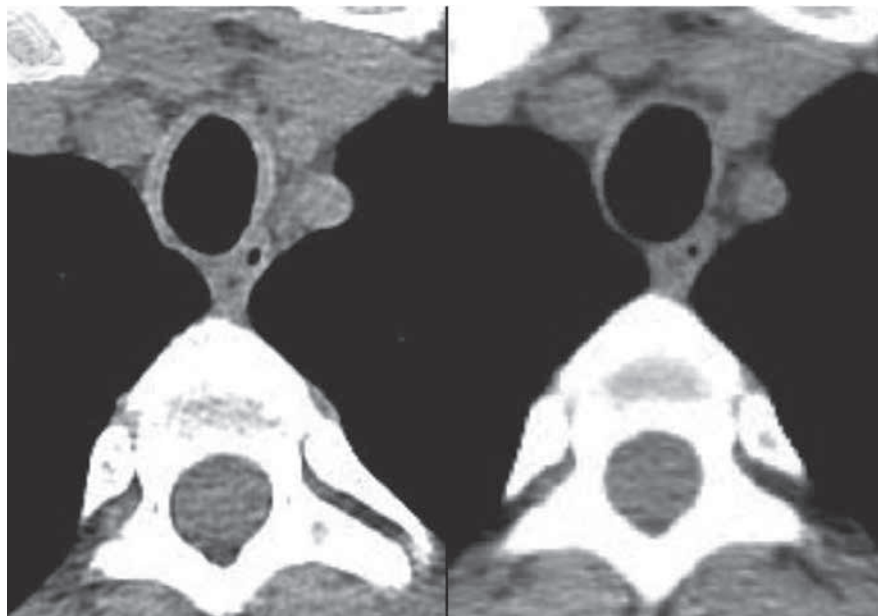

Fig. 12. — Follow-up evaluation in a patient affected by GPA with symmetrical. The circumferential tracheal involvement seen on the baseline examination (left) has totally disappeared after immunosuppressive therapy (right).

without association with a halo-sign or cavitations (very rare).

- Airway involvement is rare, consisting in centrilobular nodules, tree-in-bud pattern, bronchial dilatation,
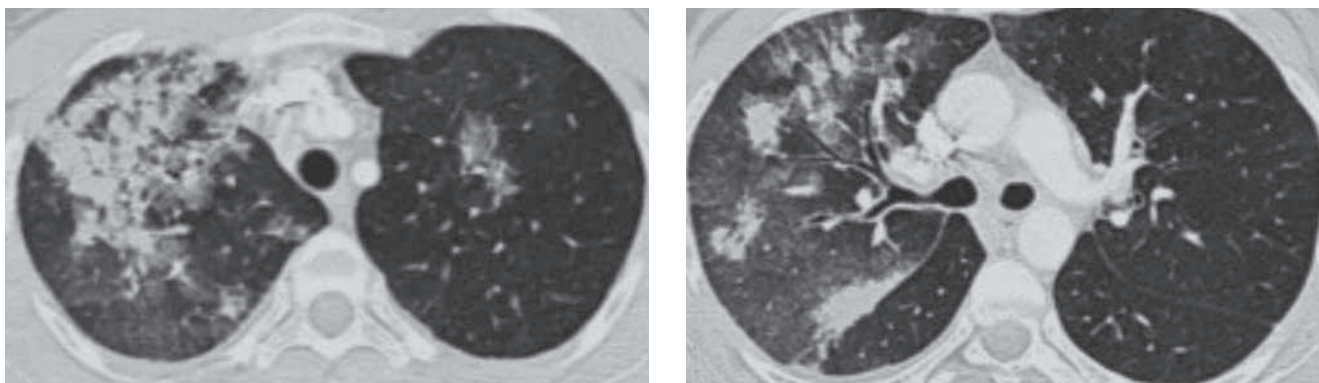
Fig. 13. — CT study in a patient with eosinophilic granulomatosis with polyangiitis (EGPA) showing areas of randomly distributed patchy areas of airspace consolidation and ground-glass opacities, mainly localized in the right upper lobe.

and bronchial and bronchiolar wall thickening. These abnormalities are related to asthma in most of the cases (which is almost always present), or, less commonly, to an eosinophilic involvement of the bronchial wall.

Unilateral or bilateral pleural effusions are relatively frequent (10%–50% of cases) and may be related to heart failure resulting from cardiomyopathy or eosinophilic pleuritis. Lymph node enlargement and pericardial effusion are uncommon findings.

Imaging follow-up

Follow-up studies after therapy show, in the majority of cases, a complete resolution of all parenchymal abnormalities (clinical remission achieved in more than 90% of patients). Airways abnormalities (bronchial wall thickening and dilatations) tend to be less reactive to treatment.

Differential diagnosis

The main radiologic differential diagnoses include other diseases that may present with transient, patchy ground-glass opacities or consolidations without any lobar predilection in patients with a history of asthma. The differential diagnosis of EGPA is essentially based on the knowledge of the systemic manifestations of disease, including rash, peripheral neuropathy and presence of serum p-ANCA.

Chronic pulmonary eosinophilic pneumonia may present radiologically with similar patterns than those of EGPA with patchy, transient and migratory non segmental ground-glass opacities or consolidations, associated with eosinophilia. The other differential diagnoses include acute allergic bronchopulmonary aspergillosis, organizing pneumonia and

infectious pneumonia, mainly represented by bacterial bronchopneumonia and opportunistic agents, such as *Pneumocystis Jirovecii* and *Cytomegalovirus* (especially in asthmatic patients under corticosteroids therapy).

Microscopic polyangiitis (MPA)

Microscopic polyangiitis is necrotizing non granulomatous vasculitis with few or no immune deposits that predominantly affects small vessels. It represents the first cause of pulmonary-renal syndrome (2,8). Its incidence is estimated at 1/100.000/year with a slight male predominance and mean age at onset of about 50 years. The main clinical features are represented by rapidly progressive glomerulonephritis (90% of cases) and diffuse alveolar hemorrhage (DAH, 10%-30% of cases). DAH can be defined by the presence of hemoptysis, diffuse alveolar infiltrates, and a drop in hematocrit level. The most common histologic finding in patients with DAH is capillaritis (17, 18).

Radiological manifestations of the disease

Imaging features of microscopic polyangiitis at CT, nonspecific, are those characterizing a DAH, with ground-glass opacities as the most common radiological manifestation.

Bilateral (less commonly even unilateral), patchy or diffuse ground-glass opacities (partial alveolar blood filling; 90% of cases), airspace consolidations (complete alveolar blood filling; 70% of cases) with no predominant distribution and thickening of the bronchovascular bundles (51% of cases). Poorly defined and centrilobular nodular areas of ground-glass opacities may be pre-

dominant in some patients, representing localized foci of hemorrhage.

After an acute episode of hemorrhage, the hemosiderin-laden macrophages accumulate in the interstitium, causing interlobular septal thickening in association with ground-glass opacity (crazy-paving pattern).

Pulmonary fibrosis is a rare but clinically relevant manifestation occurring in association with ANCA associated vasculitis, especially among patients with microscopic polyangiitis and with anti-myeloperoxydase (MPO)-ANCA specificity (19, 20). As for the other ANCA-associated vasculitides, the main pattern of pulmonary fibrosis associated with microscopic polyangiitis is usual interstitial pneumonia (UIP) (Fig. 14), but other patterns may be encountered, including non specific interstitial pneumonia (NSIP) and combined emphysema-pulmonary fibrosis (CEPF).

Pleural effusions can be detected in up to the 15% of cases; pulmonary edema in the 6% of cases

Imaging follow-up

After therapy, most of the patients show a complete resolution or a reduction of ground-glass opacities and parenchymal consolidations. Septal thickening and mild fibrotic changes may persist in severe and reiterated presentations. When interstitial lung disease is present, it progresses with worsening of fibrosis.

Differential diagnosis

The diagnosis of microscopic polyangiitis should be suspected in patients with rapidly progressive glomerulonephritis, serum p-ANCA and radiological manifestations of hemorrhage.
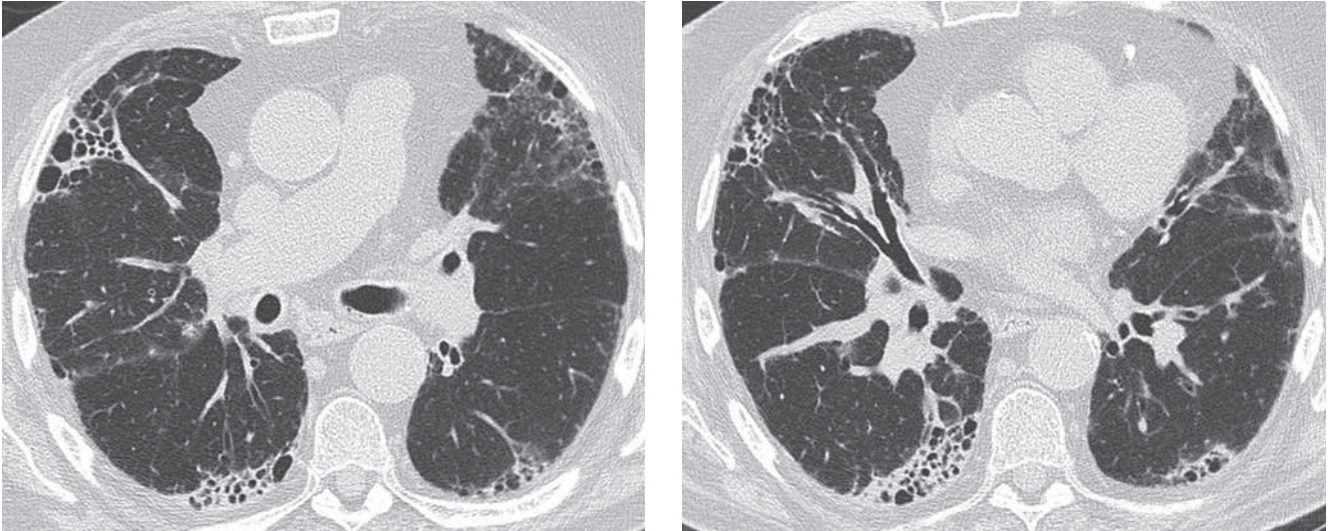
Fig. 14. — Patient affected by microscopic polyangiitis. CT scan shows bilateral subpleural honeycombing predominantly localized in the lower lobes suggestive of usual interstitial pneumonia (UIP).

The main radiological differential diagnosis comprehends all conditions possibly causing alveolar hemorrhage. Most cases of DAH are generally caused by capillaritis associated with systemic autoimmune diseases such as ANCA-associated small-vessel vasculitis, anti-GBM disease and systemic lupus erythematosus.

Hypersentivity peumonitis may be suggested when the predominant pattern is represented by centrilobular poorly defined or ground-glass nodules.

Pulmonary fibrosis is often the first manifestation of pulmonary fibrosis associated to ANCA associated vasculitis and it may precede systemic symptoms of the vasculitis by months or even years and be initially classified as idiopathic pulmonary fibrosis.

Anti-glomerular basement membrane (anti-GBM) disease

Anti-GBM disease is a vasculitis affecting glomerular capillaries, pulmonary capillaries, or both with basement membrane deposition of anti-basement membrane autoantibodies. It is regarded as an immune complex vasculitis, because the pathogenesis involves in situ formation of immune complexes between anti-GBM anti-bodies and GBM antigens with resultant activation of inflammatory mediators (2).

Anti-GBM disease is extremely rare (incidence 1/1.000.000/year), more common in men than in women with an onset between 20-30 years of age. It is characterized by anti–GBM

Fig. 15. — Patient with anti-glomerular basement membrane (anti-GBM) disease. Pulmonary hemorrhage responsible for recurrent hemoptysis. CT study demonstrates bilateral areas of ground-glass opacities having medullar distribution within the upper lobes.

antibodies (more than 90% of cases), directed against basement membrane antigens of the alveolus and glomerulus.

The most common presenting symptom is hemoptysis, sometimes lifethreatening.

Radiological manifestations of the disease

The radiological manifestations correspond to the typical imaging features of a DAH, with bilateral ground-glass opacities (Fig. 15) and less commonly areas of airspace consolidations. Ground-glass opacities may have a diffuse or patchy distribution (Fig. 15). Less commonly,

small, poorly defined homogeneously and diffusely distributed ground-glass centrilobular nodules (Fig. 16) and interlobular septal thickening can be found.

Imaging follow-up

Treatment options are given by plasmapheresis and immunosuppressive drugs (corticosteroids and cyclophosphamide). After successful treatment, imaging follow-up can show a complete resolution or reduction of ground-glass opacities and parenchymal consolidations. Septal thickening and mild fibrotic changes may persist in severe and reiterated presentations. When a CT
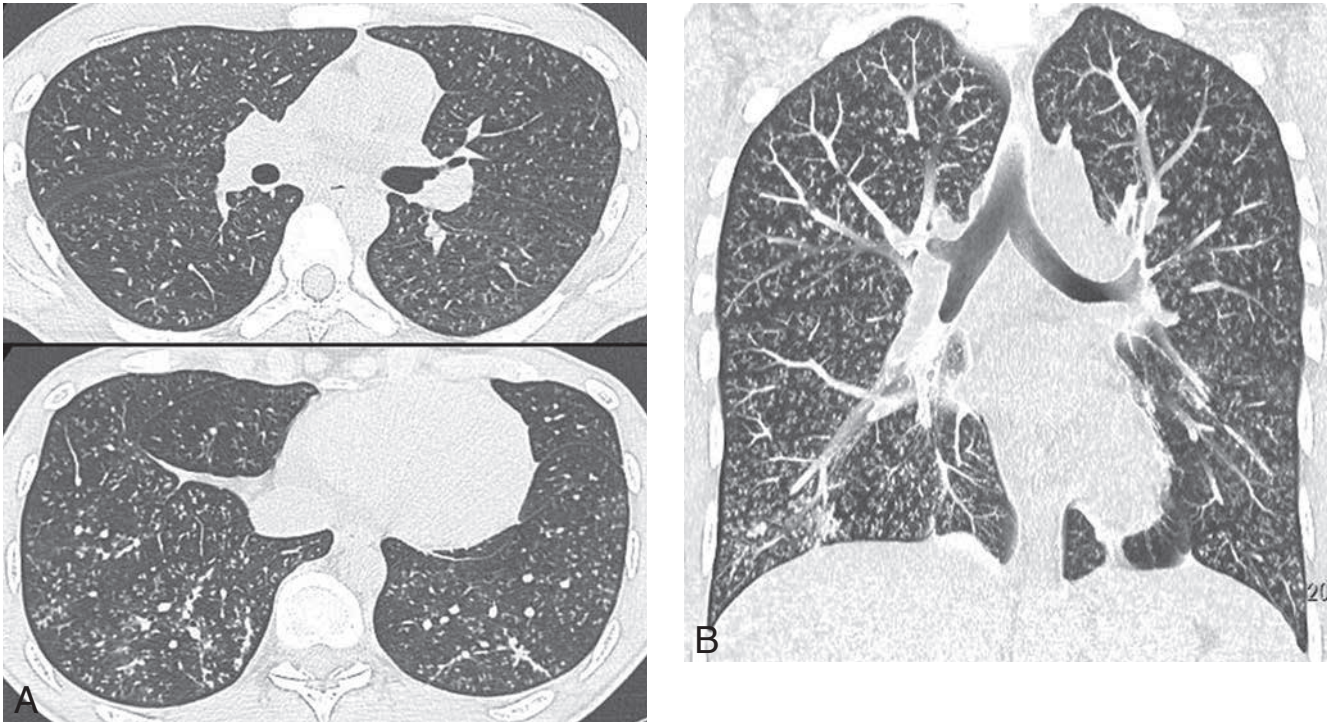
Fig. 16. — 19-year-old male patient with hemoptysis revealing an anti-GBM disease. Axial images (A) showing multiple centrilobular nodular opacities homogenously and diffusely distributed throughout the lungs. Coronal reformatted slab with maximum intensity projection (B) displaying centrilobular nodular opacities mimicking a tree in bud appearance.

scan is performed 2-3 days after the acute episode, a prevalence of the centrilobular nodules and interlobular septal thickening pattern can be found.

Differential diagnosis

Anti-GBM disease should always be suspected in a patient with hemoptysis, bilateral airspace consolidations or ground-glass opacities and renal disease. The presence of anti–GBM antibodies would confirm the diagnosis.

The radiological differential diagnosis includes all conditions which can cause pulmonary hemorrhage associated with a renal involvement, such as

connective tissue diseases (especially systemic lupus erythematosus) and ANCA-associated vasculitis (especially granulomatosis with polyangiitis and microscopic polyangiitis).

Other differential diagnoses include blood aspiration and metastasis from highly vascularized tumors, such as choriocarcinoma.

Behçet's disease

Behçet's disease is a variable-vessel vaculitis with non predominant type of vessel involved that can affect the vessels of any size (small, medium and large) and type (arteries, veins and capillaries). It is an uncommon systemic disorder (prevalence of about 1/100.000) characterized by vasculitis and a clinical triad of recurrent oral and genital ulcers and relapsing uveitis. Mean age of onset is about 30 years; men are much more commonly affected than women. Pleuropulmonary involvement is quite rare (1%-18% of cases) and mainly characterized by pulmonary arteries aneurysms, hemorrhage and parenchymal infarcts (21, 22). The main clinical manifestation is hemoptysis, sometimes massive and life threatening. The Hughes-Stovin syndrome is considered by many authors as a rare variant of Behçet's disease, characterized by systemic venous thrombi and pulmonary aneurysms and thrombosis without oral and genital ulcerations and eye involvement (23).

Radiological manifestations of the disease

Chest-CT with contrast media administration allows the evaluation of presence, location and size of pulmonary aneurysms, their possible complications (thrombosis, pulmonary infarcts) and other parenchymal and vascular associated findings.

Pulmonary aneurysms are, in the most of cases, multiple, bilateral, fusiform or saccular and their dimensions range from 1 to 7 cm in diameter (Fig. 17). The most common localization of pulmonary aneurysms is the right interlobar artery, followed by lobar and segmental arteries. The affected vessel can show signs of inflammation, as wall-thickening and wall-enhancement after contrast media administration.

Partial or complete thrombosis of the aneurysms is a frequent finding. Such occlusions can lead to localized areas of consolidations (wedge-shaped peripheral consolidations, rarely with cavitations) related to parenchymal infarctions, focal atelectasis and areas of oligemia.

Intracardiac thrombus (Kajiya T, Heart vessels 2007) has been reported.

Vasculitis and rupture of pulmonary arteries can lead to alveolar hemorrhage, with focal, patchy or diffused areas of consolidations or ground-glass opacities (Fig. 18).

Associated findings may include recurrent pneumonia and organizing pneumonia, unilateral or bilateral pleural effusions as a result of pleural vasculitis, and pulmonary infarcts or thrombosis occurring in the superior vena cava.
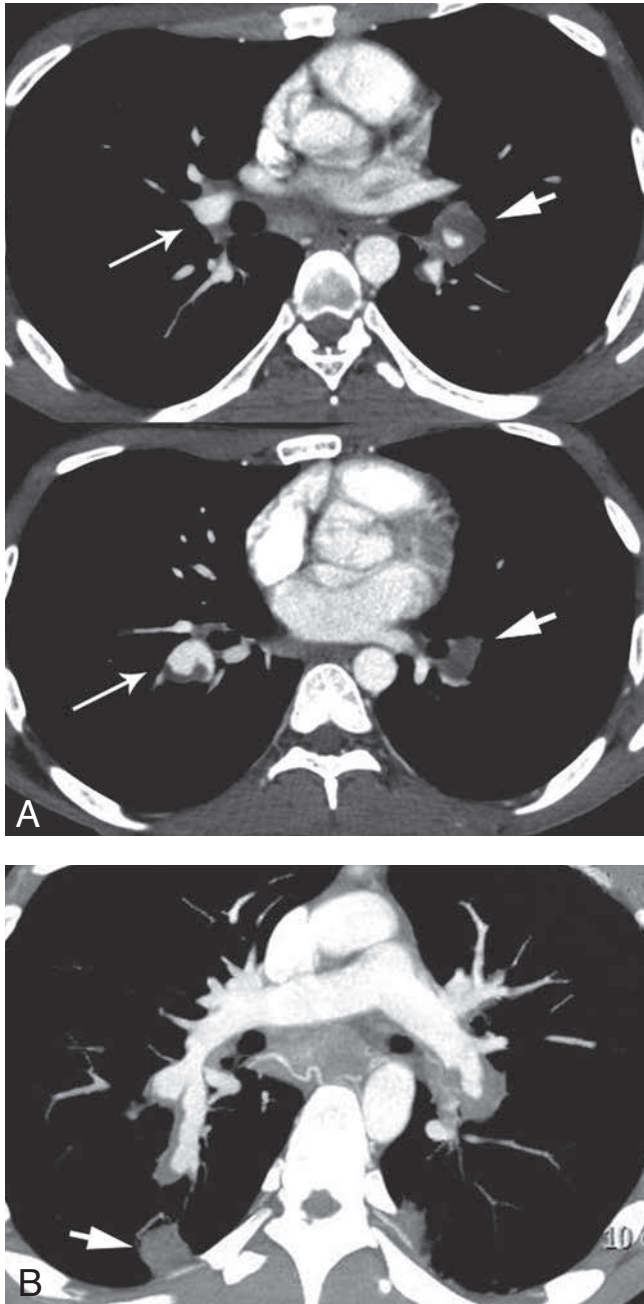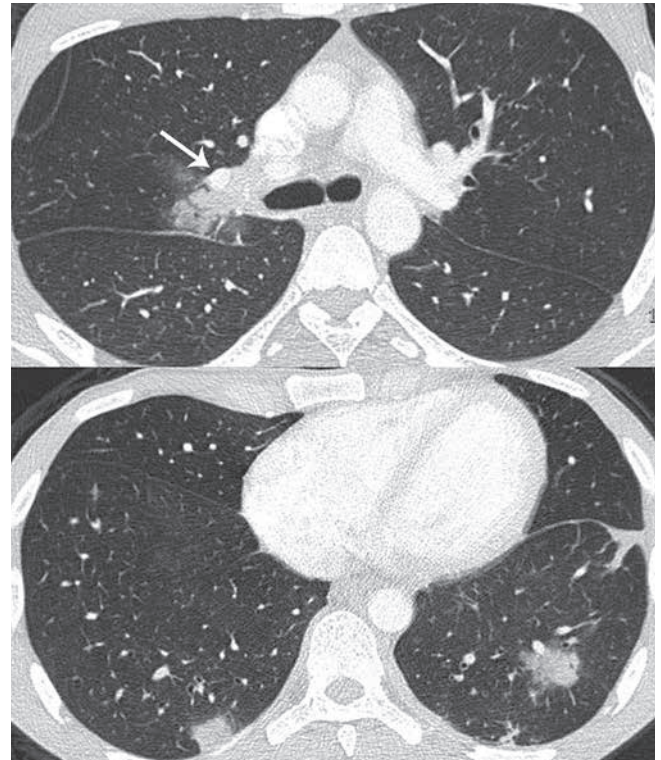
Fig. 18. — Same patient as figure 17. Lung parenchyma window settings axial images. There is a focal perihilar consolidation surrounded by ground-glass opacity at the level of the carina, next to a small aneurysm of a proximal branch of the right pulmonary artery (arrow) (top). Another focal consolidation surrounded by a ground-glass opacity and a wedge-shaped subpleural consolidation are demonstrated in the lower lobes, reflecting pulmonary hemorrhage and infarction respectively (bottom).

Fig. 17. — Patient affected by Behçet's disease. A. Axial CT images after contrast enhancement showing a partly thrombosed aneurysm of the left interlobar and lower lobar pulmonary arteries (small arrows), and aneurysm of the right interlobar pulmonary artery also partially thrombosed (long arrows). B. Maximum intensity projection reformation displaying the vascular abnormalities. Distal occlusion of the right aneurysm with a peripheral wedge-shaped consolidation, reflecting pulmonary infarction (arrow).

Imaging follow-up

Repeated scans over time allow the monitoring of aneurysms formation and the follow-up of their parenchymal complications. Patients receiving immunosuppressive treatment can show reduction or complete resolution (up to the 75% of cases) of pulmonary aneurysms and associated thrombosis (Fig. 19).

Differential diagnosis

Pulmonary artery aneurysms are an uncommon finding, which can be given by a small number of conditions, including infections (especially mycotic pseudoaneurysms), previous trauma (often iatrogenic) and Takayasu arteritis.

Takayasu arteritis

Takayasu arteritis is a large vessel vasculitis often granulomatous that predominantly affects the aorta and its major branches (2). However, any size artery may be affected. Onset is usually in patients < of 50 years of age.

The main vascular abnormalities are given by stenosis or occlusion with possible poststenotic dilatations and aneurysm formation (24,25). Distribution of lesions is usually segmental and patchy. Involvement of the pulmonary arteries can be found in about the 50%-80% of cases, as a late manifestation of disease. Although more common in Japan and Southeast Asia, the disease has been found worldwide, usually affecting young women (10-40 years old). To limit radiation exposure, MRI should
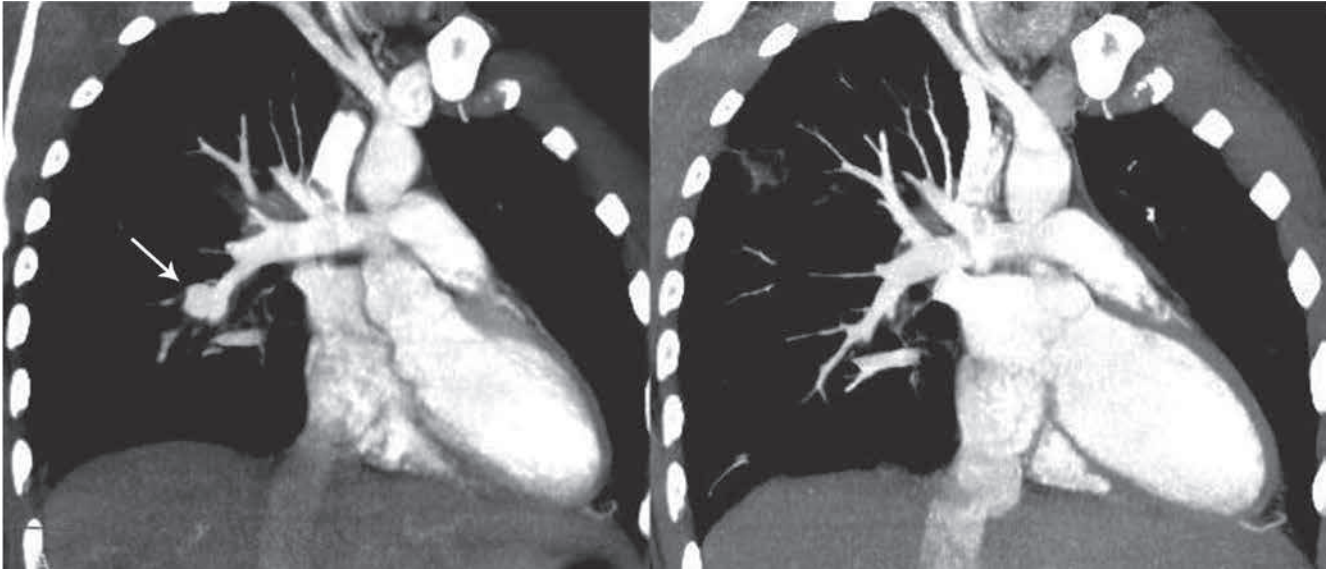
Fig. 19. — Follow-up evaluation in a patient with Behçet's disease. Left: focal pulmonary aneurysm of a right segmental pulmonary artery (arrow). Right: there is a complete resolution of the aneurysm after immunosuppressive treatment.

Fig. 21. — Patient with Takayasu arteritis. Contrast enhanced CT study showing a focal aneurysm of the pulmonary trunk (arrow).
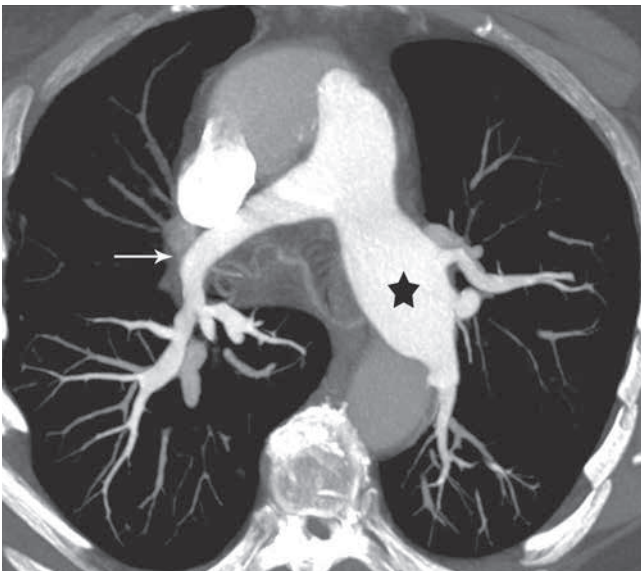
Fig. 20. — Patient with by Takayasu arteritis. CT angiography of pulmonary arteries. Axial reformatted maximum intensity projection image. Aneurysm of the left pulmonary artery (star) and a mild stenosis of the right pulmonary artery with complete occlusion of the right superior and middle branches (arrow).
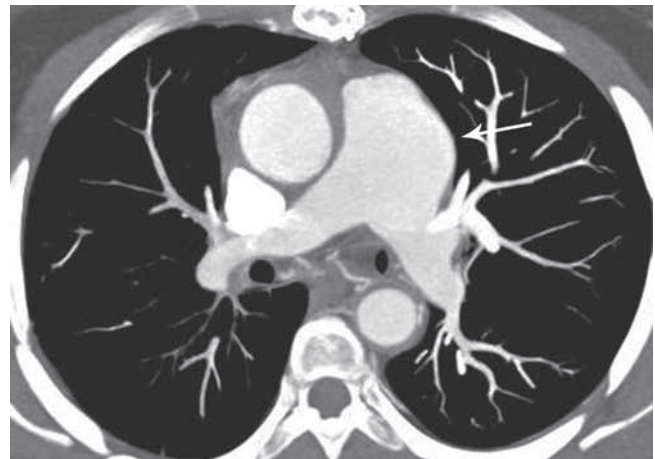
be the modality of choice in suspected or proved disease.

Radiological manifestations of the disease

The most common pulmonary manifestation of disease is given by stenosis or occlusion and aneurysm formation of segmental or subsegmental pulmonary artery branches (less commonly of the lobar or main pulmonary arteries). The most frequent localization is the right up-per lobe, followed by the middle lobe, the lingula, and the lower lobes (Fig. 20 and 21). Affected vessels can show wall-thickening and contrast-enhancement in early phases, calcium deposition in chronic phases. Vascular abnormalities can be associated to parenchymal areas of oligemia or pulmonary infarcts.

Imaging follow-up

Vascular lesions tend to progress over time. A control of disease can be achieved with high-doses of corticosteroids or with cytotoxic drugs in patients non responding to corticosteroids and with frequent relapses.

Differential diagnosis

The main differential diagnosis for the pulmonary manifestations of disease is Behçet's Disease. Integration with the clinical background of the patient and histologic findings are necessary for diagnosis.

Conclusions

Imaging features of pulmonary involvement in systemic vasculitis can be extremely heterogeneous and the differential diagnosis very challenging. Nevertheless, every

vasculitis can be characterized by peculiar combinations of clinical and radiological signs. Only the integration between the clinical, serological and pathological data derived from a close cooperation with the referring physicians and an appropriate knowledge of the specific radiological patterns of each vasculitis allows the formulation of the possible diagnosis.

Bibliography

1. Jennette J.C., Falk R.J., Andrassy K. et al.: Nomenclature of systemic vasculitides. Proposal of an international consensus conference. *Arthritis Rheum*, 1994, 37:187-192.
2. Jennette J.C., Falk R.J., Bacon P.A., et al.: 2012 Revised international Chapel Hill consensus conference nomenclature of vasculitides. *Arthritis Rheum*, 2013, 65:1-11.
3. Castañer E., Alguersuari A., Gallardo X. et al.: When to suspect pulmonary vasculitis: radiologic and clinical clues. *Radiographics*, 2010, 30:33-53.
4. Frankel S.K., Cosgrove G.P., Fischer A., Meehan R.T., Brown K.K.: Update in the diagnosis and management of pulmonary vasculitis. *Chest*, 2006, 129:452-465.
5. Foulon G., Delaval P., Valeyre D., et al.: ANCA-associated lung fibrosis: analysis of 17 patients. *Respir Med*, 2008, 102:1392-1398
6. Hansell D.M.: Small-vessel diseases of the lung: CT pathologic correlates. *Radiology*, 2002, 225:639-653.
7. Chung M.P., Yi C.A., Lee H.Y., Han J., Lee K.S.: Imaging of pulmonary vasculitis. *Radiology*, 2010, 255:322-341.
8. Marten K., Schnyder P., Schirg E., Prokop M., Rummeny E.J., Engelke C.: Pattern-based differential diagnosis in pulmonary vasculitis using volumetric CT. *AJR Am J Roentgenol*, 2005, 184:720–733.
9. Ananthakrishnan L. Sharma N., Kanne J.P.: Wegener's granulomatosis in the chest: high-resolution CT findings. *AJR Am J Roentgenol*, 2009, 192:676-682.
10. Lohrmann C., Uhl M., Schaefer O., Ghanem N., Kotter E., Langer M.: Serial High-Resolution Computed Tomography Imaging in Patients with Wegener Granulomatosis: Differentiation Between Active Inflammatory and Chronic Fibrotic Lesions. *Acta Radiol*, 2005, 46:484-491.
11. Lee K.S., Kim T.S., Fujimoto K. et al.: Thoracic manifestation of Wegener's granulomatosis: CT findings in 30 patients. *Eur Radiol*, 2003, 13:43–51.
12. Prince J.S., Duhamel D.R., Levin D.L., Harrell J.H., Friedman P.J.: Nonneoplastic lesions of the tracheobronchial wall: radiographics findings with bronchoscopic correlation. *Radiographics*, 2002, 22:S215-S230.
13. Webb E.M., Elicker B.M., Webb W.R.: Using CT to diagnose nonneoplastic tracheal abnormalities: appearance of the tracheal wall. *AJR Am J Roentgenol*, 2000, 174:1315-1321.
14. Attali P., Begum R., Ban Romdhane H., Valeyre D., Guillevin L., Brauner M.W.: Pulmonary Wegener's granulomatosis: changes at follow-up CT. *Eur Radiol*, 1998, 8:1009-1013.
15. Worthy S.A., Müller N.L., Hansell D.M., Flower C.D.: Churg-Strauss syndrome: the spectrum of pulmonary CT findings in 17 patients. *AJR Am J Roentgenol* 1998, 170:297–300.
16. Silva C.I., Müller N.L., Fujimoto K., Johkoh T., Ajzen S.A., Churg A.: Churg-Strauss syndrome: high resolution CT and pathologic findings. *J Thorac Imaging,* 2005, 20:74–80.
17. Primack S.L., Miller R.R., Müller N.L.: Diffuse pulmonary hemorrhage: clinical, pathologic, and imaging features. *AJR Am J Roentgenol*, 1995, 164:295–300.
18. Cortese G., Nicali R., Placido R., Gariazzo G., Anrò P.: Radiological aspects of diffuse alveolar haemorrhage. *Radiol Med*, 2008, 113:16-28.
19. Tzelepis G.E., Kokosi M., Tzioufas A. et al.: Prevalence and outcome of pulmonary fibrosis in microscopic polyangiitis. *Eur Respir* J, 2010, 36:116-121
20. Hervier B., Pagnoux C., Agard C., et al.: Pulmonary fibrosis associated with ANCA-positive vasculitides. Retrospective study of 12 cases and review of the literature. *Ann Rheum Dis*, 2009, 68:404-407.
21. Chae E.J., Do K.H., Seo J.B., et al.: Radiologic and clinical findings of Behçet disease: comprehensive review of multisystemic involvement. *RadioGraphics*, 2008, 28:e31.
22. Hiller N., Lieberman S., Chajek-Shaul T., Bar-Ziv J., Shaham D.: Thoracic manifestations of Behçet disease at CT. *Radiographics*, 2004, 24:801-808.
23. Emad Y., Ragab Y., Shawki Ael-H., Gheita T., El-Marakbi A., Salama M.H.: Hughes-Stovin syndrome: is it incomplete Behçet's? Report of two cases and review of the literature. *Clin Rheumatol*, 2007, 26:1993-1396.
24. Paul J.F., Hernigou A., Lefebvre C., et al.: Electron beam CT features of the pulmonary artery in Takayasu's arteritis. *AJR Am J Roentgenol*, 1999, 173:89-93.
25. Park J.H., Chung J.W., Im J.G., Kim S.K., Park Y.B., Han M.C.: Takayasu arteritis: evaluation of mural changes in the aorta and pulmonary artery with CT angiography. *Radiology*, 1995, 196:89–93.